



HAL
open science

Promising potential of bio-sourced amphiphilic xanthan as an emulsifier in O/W dispersions

Mira Abou Dib, Marie Lemarchand, Ecaterina Gore, Michel Grisel

► To cite this version:

Mira Abou Dib, Marie Lemarchand, Ecaterina Gore, Michel Grisel. Promising potential of bio-sourced amphiphilic xanthan as an emulsifier in O/W dispersions. *Colloids and Surfaces A: Physicochemical and Engineering Aspects*, 2023, 663, pp.131062. 10.1016/j.colsurfa.2023.131062 . hal-04767788

HAL Id: hal-04767788

<https://hal.science/hal-04767788v1>

Submitted on 12 Nov 2024

HAL is a multi-disciplinary open access archive for the deposit and dissemination of scientific research documents, whether they are published or not. The documents may come from teaching and research institutions in France or abroad, or from public or private research centers.

L'archive ouverte pluridisciplinaire **HAL**, est destinée au dépôt et à la diffusion de documents scientifiques de niveau recherche, publiés ou non, émanant des établissements d'enseignement et de recherche français ou étrangers, des laboratoires publics ou privés.

Copyright

Promising potential of bio-sourced amphiphilic xanthan as an emulsifier in O/W dispersions

Mira Abou Dib*, Marie Lemarchand, Ecaterina Gore, Michel Grisel*

Normandie Univ, UNILEHAVRE, FR 3038 CNRS, URCOM, 25 rue Philippe Lebon, BP 1123, 76063 Le Havre cedex, France

*corresponding author: michel.grisel@univ-lehavre.fr and mira.aboudib.27@gmail.com

Abstract

The emulsification properties of hydrophobically modified xanthan (HMX) obtained through green esterification using alkenyl succinic anhydrides (ASA) as grafting agents were investigated by preparing oil-in-water emulsions without adding any surfactant, in order to better understand the stability phenomenon at the oil-water interface. This study demonstrated that new-brand bio-sourced HMX owns emulsifying potential compared to pristine xanthane, known for its poor interfacial properties as a non-absorbing polymer. A complete approach for studying the stability of the dispersions was carried out at different levels: a) macroscopic level: visual identification of stability, b) microscopic level: coupled optical microscopy and droplet size distribution and c) deep microstructure stability monitoring over time by Static Multiple Light Scattering. First, a series of HMX differing in alkenyl chain length and grafting density added at 0.2% w/w in emulsions were compared. Increased grafting density or hydrophobic chain length provided a highly stable and homogeneous emulsion over 30 days. In the case of less stable emulsions, two solutions are proposed: 1) increasing HMX concentration thus improving emulsifying properties, 2) adding native xanthan as a thickening agent, which slows down the creaming destabilization mechanism. This original article shows that the new-brand bio-sourced amphiphilic xanthan obtained under green modification synthesis behave promising and effective emulsifying capacities to stabilize oil-in-water emulsions, which offers promising potential for industrial applications.

Keywords

Amphiphilic xanthan, green modification, oil-in-water dispersion, stabilization, emulsification properties

1. Introduction

Emulsions are widely used and developed in multiple industrial fields such as foods [1], cosmetics [2], pharmaceuticals [3] and agrochemicals [4]. They are thermodynamically unstable mixtures made of two or more immiscible liquids [5]; oil-in-water (O/W) emulsions consist of oil droplets dispersed in a continuous aqueous phase. Since the contact between oil and water is energetically unfavorable, O/W emulsions tend to undergo destabilization processes over time such as creaming, flocculation, coalescence and Ostwald ripening; thus leading to the oiling off and the emulsion breaks up into phase separation [6,7]. However, it is possible to kinetically stabilize emulsions by adding additional components that can be: a) thickening agents such as polysaccharides that slow down droplets motion and breaking phenomenon thanks to their ability to increase viscosity of aqueous phase [8] and b) emulsifiers such as surfactants [9], solid particles [10] or polymeric surfactants [11–13]. In fact, the

39 emulsifier can adsorb at the oil-water interface providing a protective barrier that prevents or slows
40 coalescence, ensuring long-term stability. Among polymeric surfactants, despite their high interest due
41 to natural origin, there is only a limited number of polysaccharides naturally owning surface activity
42 and emulsifying properties such as Arabic gum [14], talha gum [15], mesquite gum [16] and certain
43 galactomannans such as guar, locust bean [17,18], and fenugreek gum [19,20] which surface activity
44 was attributed to the hydrophobic protein component that anchor strongly the oil-water interface,
45 while the hydrophilic hydrocolloid chains form protective layer providing steric stabilization [11]. Many
46 other polysaccharides lack surface activity and do not exhibit adsorbent character so they cannot bring
47 any interfaces stabilization. To deal with this poor interfacial properties of such hydrocolloid, multiple
48 studies were developed on hydrophobically modification of polysaccharides based on the pioneering
49 work of Landoll [21] to endow them with interfacial properties. Among other polysaccharides, xanthan
50 is well known for its outstanding viscosifying capacities that can lead to dispersions stabilization due
51 to thickening effect of the continuous phase [22]. Nevertheless, its poor interfacial properties prevent
52 it to long-term stabilize dispersions without adding conventional surfactants; however these latter
53 compounds own negative toxicological and environmental impacts [23,24].

54 Recent literature studies have shown that ASA-modified polysaccharides have different potential
55 applications mainly encapsulation, emulsification and stabilization [25–29]. In addition, one of them
56 was approved as additive in food and medicine by the Food and Drug administration, it is the octenyl
57 grafted starch (OSA-starch) [30].

58 In a previous work, a variety of amphiphilic xanthan derivatives were prepared via green esterification
59 reaction between xanthan and a series of alkenyl succinic anhydride (ASA) as grafting agents [31]. The
60 study allowed revealing optimized conditions to obtain high grafted xanthan with three different
61 alkenyl chain length, namely octenyl, dodecenyl and hexadecenyl; it also highlighted the surface
62 activity enhancement of the xanthan when grafted with long alkenyl chain or high rate of hydrophobic
63 moieties.

64 The present work details the potential for amphiphilic xanthan derivatives to emulsify dispersions
65 without adding any low molecular weight surfactant. The study first focuses on the effect of the
66 grafting density and the grafted chain length on the potentiality to stabilize O/W emulsions. Then, the
67 impact of HMX concentration as well as its synergy with native xanthan is described. Properties of all
68 emulsions was evaluated and compared over time in order to understand the phenomenon governing
69 the emulsions stability.

70 **2. Materials and methods**

71 **2.1. Materials**

72 Xanthan gum sample was kindly given by Cargill (France) and characterized in terms of moisture
73 content (11.3% w/w), protein content (0.95% w/w) and substitution degrees of acetate and pyruvate
74 per monomeric unit, 0.56 and 0.59 respectively [31]. Hydrochloric acid (HCl) was purchased from Fisher
75 Scientific (USA), sodium chloride (NaCl) from Carlo Erba and sodium azide (NaN₃) used as preservative
76 against bacteria growth was from Sigma Aldrich (USA). Ultra-pure water (16.8 MΩ.cm resistivity) was
77 used as solvent for all preparations. For emulsion preparation, isononyl isononanoate (ININ) was used
78 as oil phase with a density of 0.856 g/cm³, it was kindly offered by Stéarinerie Dubois (France). All
79 chemical reagents were analytical grades.

80 2.2. Synthesis of hydrophobically modified xanthan

81 Hydrophobically modified xanthan HMX samples were obtained via a succinylation reaction of xanthan
82 using 2-Octen-1-ylsuccinic anhydride (OSA), (2-Dodecen-1-yl) succinic anhydride (DDSA) or
83 Hexadecenyl succinic anhydride (HDSA) based on a procedure according to [31].

84 As fully described in a previous study, reaction optimization was performed for each HMX derivatives
85 (C8, C12 and C16) by varying either the reaction pH range, the reaction time and the grafting reagents
86 molar excess thus allowing accurate control of degree of succinylation (DS) up to 16 %, as determined
87 by ¹H NMR analysis [31]. All HMX used in this study remained fully water soluble thus allowing pouring
88 back in water. Resulting HMX were noted as XC8, XC12 and XC16 for octenyl-grafted, dodecenyl-
89 grafted and hexadecenyl-grafted xanthan, respectively, followed by their DS value. As an example, a
90 xanthan modified by OSA with a DS of 4.1 % will be noted as XC8(4.1). Pristine xanthan (PX) refers to
91 samples subjected to the same treatment apart from adding OSA, DDSA or HDSA. Native xanthan (NX)
92 represent the xanthan commercial batch.

93 2.3. Protocol for O/W emulsion preparation

94 Emulsions preparation was adapted from the optimized protocol previously developed in our
95 laboratory for preparing small emulsions quantities with efficient and reliable procedure [32]. Thereby,
96 it was possible to prepare in a controlled and perfectly reproducible manner 20 g of O/W emulsion
97 containing of 20 % (w/w) of oil phase (w/w) dispersed in 80 % (w/w) of aqueous phase. The mass
98 composition of the emulsions is detailed in Table 1.

99 For the aqueous phase, xanthan (native, pristine or modified) was first dissolved at concentration
100 ranging from 0.25 to 0.625 % w/w in ultrapure water under magnetic stirring at room temperature
101 overnight. Afterwards, sodium azide NaN₃ used as preservative is added at 300 ppm in the solution to
102 avoid any bacterial contamination. Then, the pH was adjusted to 4.3 by adding 0.1 M HCl and the ionic
103 strength to 1 mS/cm with NaCl(s).

104 Then, the fatty phase solely consisting of ININ oil was gently poured into the aqueous phase. The two
105 immiscible phases were heated in a water bath at 30°C in order to fully control the temperature of the
106 dispersion process. Once 30°C was reached, the mixture was homogenized for 3 minutes at 20 000
107 RPM using a T25 digital Ultra-Turrax (IKA, Germany) equipped with the dispersion head S25N-10G.
108 Resulting dispersion was then immediately degassed under vacuum in order to eliminate the air
109 incorporated during the homogenization process prior to any analysis.

110 Each dispersion was prepared in duplicate in order to verify the protocol control and reliability, and
111 also to get sufficient dispersion quantity to allow performing a series of physicochemical
112 characterizations and complementary studies.

113 *Table 1 : Composition of the formulation*

Product	Content % (w/w)	Phase
Isononyl isononanoate ININ	20	Oil
Xanthan (NX, PX or HMX)	0.2 to 0.5	Aqueous
Preservative NaN ₃	0.025	
Ultrapure water	QS	

114 2.4. Methods for the characterization of dispersions

115 On the one hand, a study based on visual macroscopic identification of stability/separation followed
116 by the microstructure observation and analysis of both droplet size and distribution in every identified
117 zone was assessed over the whole period of ageing. From a general point of view, emulsions carried
118 out with xanthan derivatives generally showed macroscopic phase separation into two phases: an
119 aqueous lower phase and an emulsified upper phase. In some cases, mixtures showed a third upper
120 phase consisting of non-emulsified supernatant oil.

121 On the other hand, an optical automated study of the entire volume of dispersion was considered by
122 analyzing the percentage of transmitted and backscattered light through dispersion as obtained by
123 Static Multiple Light Scattering measurement. Such an experimental approach allowed monitoring and
124 then understanding the different destabilization phenomenon involved in emulsions ageing, namely
125 creaming, flocculation and coalescence, thus being complementary from visual and microscopic
126 observations of the dispersions.

127 Characterizations was made directly after emulsification (D0) then over time (up to 30 days). The
128 designation D(i) will be applied referring to (i) the day of the characterizations. Only selected days are
129 showed in this article. Samples were stored at 20 °C for the entire duration of the study.

130 2.4.1. Macroscopic observations

131 The macroscopic aspect of the emulsions was followed by digital photographs just after formulation
132 and over time. Thus, it is possible to evaluate the emulsifying capacity of HMX and to detect the
133 macroscopic destabilization phenomena during aging.

134 2.4.2. Optical microscopy

135 Emulsion microstructure was observed, at room temperature with an optical microscope at a
136 magnification ranging from x100 up to x400 (ECLIPSE Ni-U NIKON, Japan) equipped with a camera DS-
137 Fi3 (5.9 megapixels CMOS image sensor). The NIS-Elements L imaging software was used to analyze
138 the photomicrograph.

139 2.4.3. Droplets size distribution

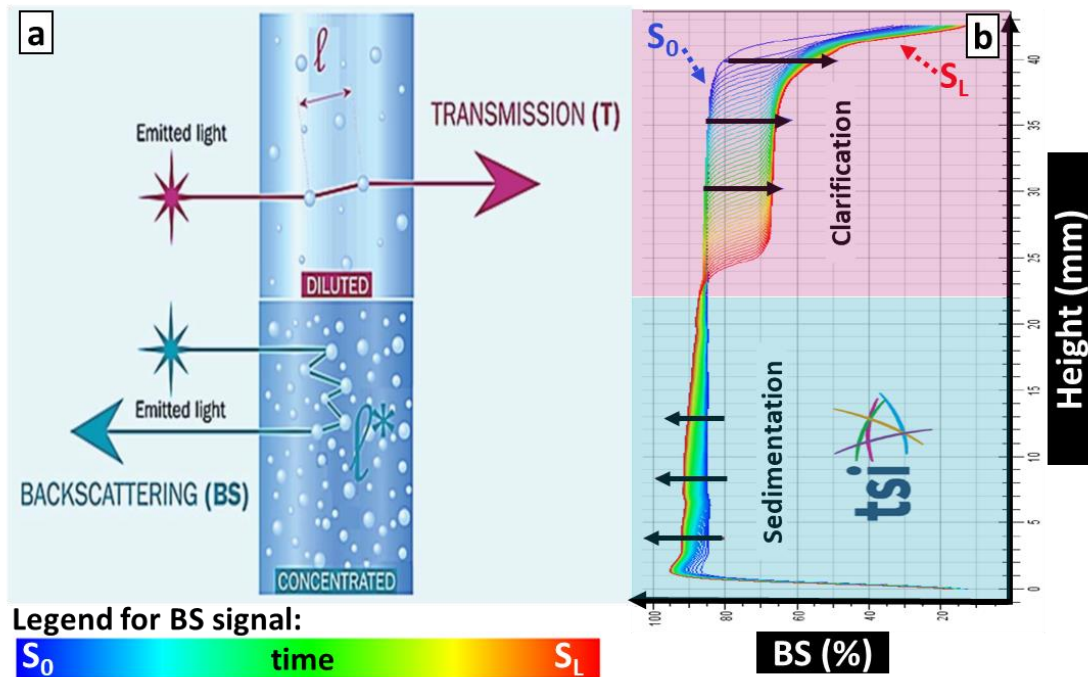
140 Emulsion droplets size was measured by static light scattering using a laser diffraction particle size
141 analyzer SALD-7500 nano (Shimadzu, Japan) equipped with a violet semi-conductor laser (405 nm) and
142 a reverse Fourier optical system. In order to study destabilization phenomena, a volume of
143 approximately 5 µL taken from the center of each of zone described above (upper and lower) was
144 diluted in ultrapure water prior to measurement in order to achieve absorption parameter within the
145 interval between 0.16 and 0.20. Sample was homogenized in the measuring batch cell (7 mL) using
146 mechanical stirring. Three repetitions were performed for each measurement using Fraunhofer's
147 theory. Data were analyzed using software Wing SALD II. Characterizations of the upper part of the
148 sample leads to a study of emulsion droplets size evolution during aging. However, characterizations
149 of the lower part were only used to confirm that less droplets remain in this separated phase.

150 2.4.4. Stability of the dispersion by Static Multiple Light Scattering technique (SMLS)

151 The stability of O/W emulsions is also characterized by the backscattering (BS) and transmission (T) of
152 a pulsed near infrared light (880 nm) by Turbiscan™ Tower (Formulation, France) which is a technique

153 based on multiple light scattering. The basic principle for such an apparatus is as follow: standardized
 154 glass tube containing the sample is locally illuminated by infrared light moving on the entire sample
 155 height from the bottom to the top of the volume; two synchronous optical sensors respectively
 156 receive: on the one hand the light transmitted through the dispersion at 180° angle from the incident
 157 light (T detector), and on the other hand light scattered backward by the dispersion at 45° from the
 158 incident radiation (BS detector) (Figure 1a). Both the collected T and BS data allow the detection of the
 159 migration phenomena of droplets and their size changings in dispersion revealing the presence of the
 160 different types of destabilization processes currently corresponding to droplets flocculation,
 161 coalescence, creaming and/or sedimentation which lead to a phase separation [33]. In general,
 162 transmission is used to analyze clear to turbid dispersions and backscattering to analyze opaque and
 163 concentrated dispersions.

164 The BS profile (vertical view) in Figure 1b shows an increase of BS in the low concentrated zone of the
 165 sample while a decreasing of BS indicating clarification corresponds to the top diluted zone. Such
 166 behaviors are proper to the sedimentation of droplets. The T profile might show opposite variation in
 167 each zone of the same sample (profile not shown to ensure clarity).



168
 169 *Figure 1: a) Work principle of SMLS-TURBISCAN™ Tower: glass tube containing dispersion with b) backscattering profile (vertical view)*
 170 *showing sedimentation phenomena (right), adapted from [12,34]*

171 Both the transmitted (T) and backscattered (BS) flux, are related to the photon mean path length λ
 172 and mean free path λ^* , respectively, as follows [34,35]:

173
$$T = T_0 e^{-\frac{2r_i}{\lambda}} \quad (1)$$

174
$$\lambda(d, \varphi) = \frac{2d}{3\varphi Q_s} \quad (2)$$

175
$$BS = \frac{1}{\sqrt{\lambda^*}} \quad (3)$$

176
$$\lambda^*(d, \phi) = \frac{\lambda}{1-g} = \frac{2d}{3\phi(1-g)Q_s} \quad (4)$$

177 Where:

- 178 - r_i is the internal radius of the measurement cell;
 179 - T_0 is the transmittance of the continuous phase;
 180 - d and ϕ are the mean diameter and the volume fraction of droplets, respectively;
 181 - g is the asymmetry factor and Q_s corresponds to the scattering efficiency factor (both are
 182 optical parameters given by the Mie theory).

183 Immediately after dispersion preparation, standardized measuring cylindrical glass cells was filled with
 184 15 g samples to be analyzed at 20 °C. The entire height of the studied samples was scanned over time
 185 (D0 to D30). Results were registered by TowerSoft (version 2.0.0.9). Both the transmitted and
 186 backscattered profiles along the height of the cell were collected as raw data.

187 Emulsion stability can be estimated using the Turbiscan Stability Index (TSI) as proposed by the
 188 software. TSI compares each scan (i) to the previous one ($i - 1$) at a selected height (h), thus dividing
 189 the result by the total height(H) as indicated below [34,36]:

190
$$TSI = \sum_i \frac{\sum_h |Scan_i(h) - Scan_{i-1}(h)|}{H} \quad (4)$$

191 Thus, TSI index gives access to the kinetic of the destabilization; it was conceived to simplify the
 192 comparison between samples. Therefore, the lower the TSI value at a particular time, the more stable
 193 is the dispersion.

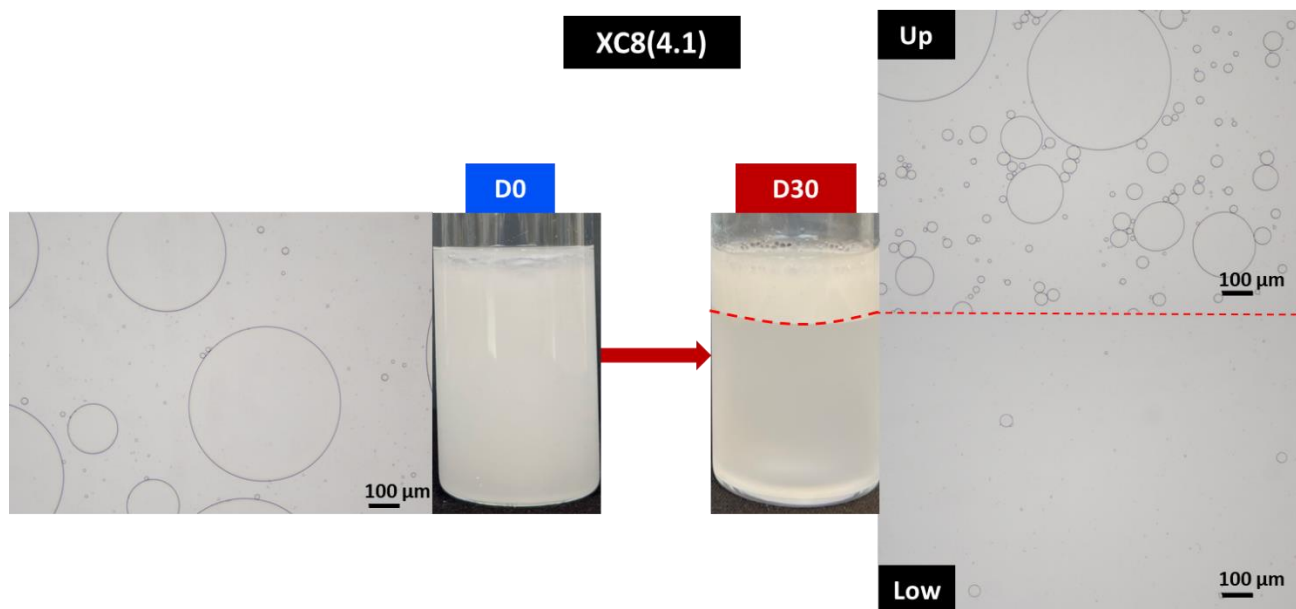
194 Among other advantages when compared to other optical methods currently used (including some
 195 used in the present paper), SMLS technique is a non-destructive method (no sampling or dilution), it
 196 detects destabilization phenomenon at a very early stage allowing to shorten aging tests and it
 197 provides together the identification of particle migration (creaming, sedimentation) and variation size
 198 variation or aggregation (flocculation, coalescence) [35].

199 3. Results and discussion

200 3.1. Evaluation of the emulsifying capacity

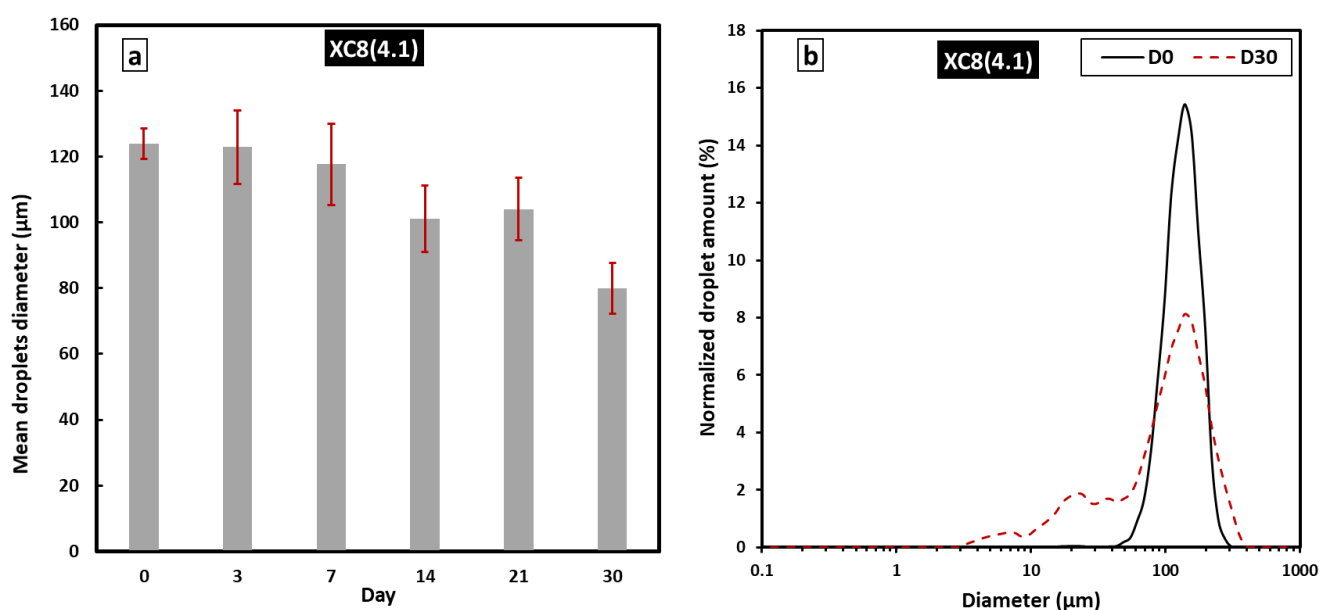
201 First, preliminary experiments using 0.2% of pristine xanthan in the O/W mixture demonstrated as
 202 expected that no emulsion stabilization was obtained, thus leading to a spontaneous phase separation.
 203 In fact, no droplets were detected by microscopic analysis immediately after the preparation process.
 204 This result is similar to that also obtained with native xanthan confirming that xanthan behaves as a
 205 non-absorbing polysaccharide due to poor interfacial properties [37,38]. However, when replacing PX
 206 by XC8(4.1), a low grafted xanthan modified with a short alkenyl chain, one can notice that emulsion
 207 was formed on the entire height of the mixture, showing large droplets as evidenced by optical
 208 microscopy image as illustrated by Figure 2. Indeed, at D0 the emulsion looks white and homogeneous
 209 from a macroscopic point of view with almost all the fatty phase dispersed in the aqueous phase.
 210 However, a thin supernatant layer of oil was rapidly observed indicating insufficient emulsifying
 211 capacity of this HMX sample at the studied concentration (0.2%). The study of the system after 24 h
 212 showed obvious phase separation with mainly two distinct phases: an upper white one for roughly 1/3

213 of the mixture height and a lower turbid one with $\frac{2}{3}$ of the height (images not shown). After one month,
 214 one can see that the two phases remained present with almost the same phases proportions as
 215 observed after 1 day, thus indicating good creaming stability during storage (Figure 2). The
 216 microstructural monitoring of both phases from D0 to D30 showed that no droplets remains in the
 217 lower phase, corresponding to the aqueous one; on the contrary within the upper emulsified phase,
 218 oil droplets of heterogeneous size still remained dispersed.



219
 220 *Figure 2 : Photographs and optical microscopy image of emulsion at 0.2% w/w XC8(4.1) at D0 and D30*

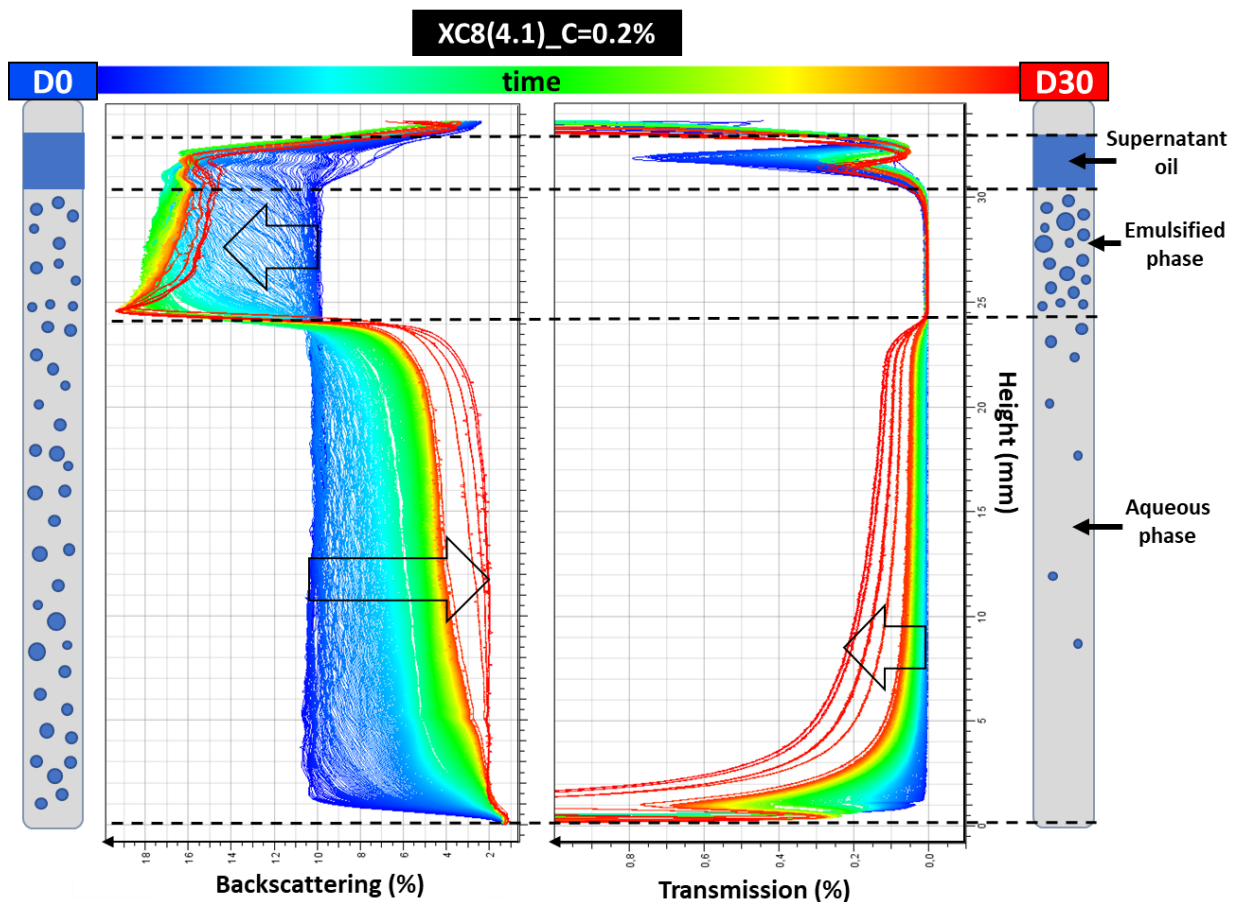
221 One can also note that when compared to the microscopic image at D0, the one at D30 showed a
 222 higher number of smaller droplets which was confirmed by a decrease of the mean diameter
 223 determined by static light scattering measurements performed for the emulsified phase over time
 224 (Figure 3a). This may simply result from the migration of droplets from the bottom to the top
 225 corresponding to the presence of creaming phenomenon.



226
 227 *Figure 3 : Evolution of: a) mean droplets diameter of the emulsified phase at different time after preparation, b) droplets size*
 228 *distribution at D0 and D30; for emulsion at 0.2% w/w XC8(4.1)*

229 In order to better understand the microstructure destabilization, it was necessary to analyze the entire
230 graphs of droplets size distribution of the emulsified phase. As presented in Figure 3b, the size
231 distribution of the emulsified phase, initially monomodal and monodisperse (D0), becomes multimodal
232 after aging with a polydisperse distribution (D30). This can be explained by two simultaneous
233 mechanisms: 1) the flocculation of the droplets as a consequence of spontaneous instability (i.e.
234 insufficient number of HMX absorbing chains present at the oil-water interface and lack of electrostatic
235 repulsions between the droplets) and 2) the creaming from the bottom to the top with gravitational
236 migration of almost all droplets including the smaller ones, into a restricted volume ($\frac{1}{3}$ of the height)
237 corresponding to the oil concentrated phase. Nevertheless, the resulting heterogeneous distribution
238 of stabilized droplet as evidenced through granulometric measurements clearly confirms the
239 microscopic visualization.

240 All these observations allow drawing hypothesis on the destabilization phenomenon that could have
241 occurred in the system. However, the need for more precise method remains essential to check the
242 interpretations. To this purpose, Turbiscan™ tower was used to allow a monitoring over short periods
243 (until 1 scan every 2 minutes) of the entire XC8(4.1) dispersion height; resulting backscattering and
244 transmission signals are presented in Figure 4. Analyzing both BS and T profiles at D0 (first blue curve)
245 showed constant value of BS and no transmission percentage over 30.5 mm height thus indicating
246 mainly homogeneous distribution of the emulsion. Then for the upper 2.5 mm, a decrease of BS and
247 an increase of T were observed, revealing a clarification due to the supernatant oil phase; these results
248 allow confirming the interpretation described above based on visual observation. Afterwards the
249 monitoring over 1 month allows the identification of two principle behaviors: first, a decrease of BS
250 (up to 2%) together with an increase of T below 24.5 mm height indicating a clarification of the lower
251 aqueous phase; simultaneously, an increase of BS with no transmission indicating an opacification of
252 the upper emulsified phase (24.5-30.5 mm). Both simultaneous phenomena clearly allow
253 demonstrating the progressive occurrence of creaming destabilization mechanism. Concerning, the
254 upper thin zone [30.5-33 mm], so-called supernatant oil phase, it would be difficult to delimit it
255 precisely because it is located between the emulsified active phase and the meniscus.



256
257
258

Figure 4 : Raw backscattering and transmission data obtained by following the evolution with time of the destabilization of the emulsion formed with XC8(4.1) at 0.2% w/w. The sample was scanned over 30 days with different scan periods

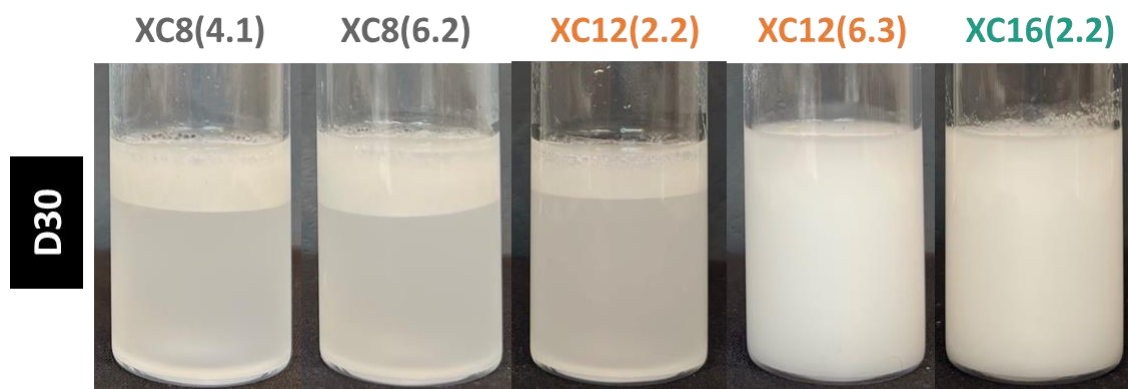
259 In this first section, the emulsifying capacity of a single HMX sample was evidenced and the
260 destabilization phenomenon governing the evolution of the dispersion over time were analyzed and
261 interpreted. In fact, the interface stabilizing character of this specific HMX owning low DS (4.1%) of
262 short alkyl residues (octyl) remains insufficient in the tested conditions (polymer concentration of 0.2%
263 w/w) to get full stabilization of the dispersion. So, next sections will aim studying the impact of each
264 parameter, namely DS, alkyl chain length and polymer concentration, on improving the emulsifying
265 potential.

266 3.2. Impact of DS and alkenyl chain length on emulsifying capacity

267 In this part, all emulsions were prepared using HMX at 0.2% (w/w) with varying both DS and alkenyl
268 residue. In these conditions all emulsions appeared white and homogeneous upon preparation
269 procedure. Both macroscopic and microstructure aspects were determined and monitored over 30
270 days in order to investigate the ability for HMX to get long-term stability emulsion in thus allowing
271 comparing all systems together.

272 Only photographs corresponding to D30 for all mixtures were presented and compared in order to
273 visualize the corresponding macroscopic stability over 1 month (Figure 5). One can notice for XC8 that
274 using HMX owning a higher DS (6.2% rather than 4.1%) do not significantly improve its emulsifying
275 capacity. Nevertheless, using XC12 instead of XC8 with keeping constant DS (6.2-6.3%) clearly allows
276 reaching much higher stability as the entire volume of the dispersion appears emulsified from a
277 macroscopic point of view. Same observation was obtained with XC12(16.9) (results are not shown to

278 keep clarity). However, it is striking that, below a certain DS, XC12 does not bring sufficient emulsifying
279 potential to stabilize the entire system in the studied conditions (C=0.2%), as illustrated for XC12(2.2)
280 in Figure 5. Finally, utilizing HMX grafted with long alkenyl chains (C16), although the grafting density
281 is low (DS = 2.2%), allows obtaining a macroscopically stable emulsion.



282
283 *Figure 5 : Photographs of emulsions at 0.2% w/w of HMX with different alkenyl chain length and grafting densities*

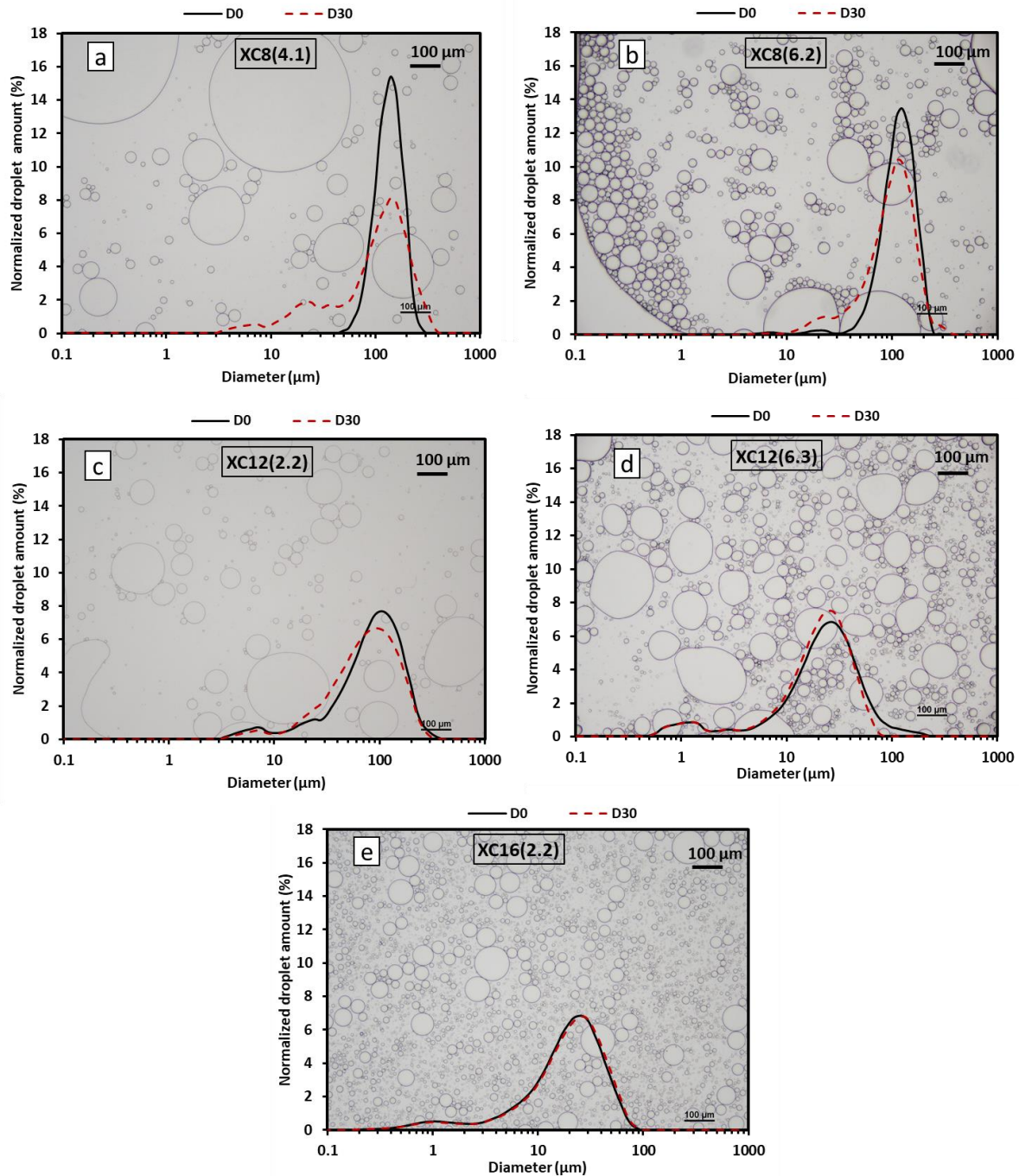
284 It is obvious that macroscopic observations cannot be sufficient for understanding and interpreting the
285 mechanisms responsible for emulsions stability with varying HMX structure. Thus, the same methods
286 for investigation as the one used for section 1 of this paper were envisaged in order to allow accurate
287 interpretations on the basis of microstructure considerations. Indeed, Figure 6 gives the optical
288 micrographs of emulsified phase at D30 superimposed with the droplet size distributions graphs for
289 the series of emulsions at different aging stages, D0 and D30 respectively.

290 Comparing microphotographs shows that all samples present droplets in the emulsified phase 30 days
291 after the dispersion preparation, thus confirm that HMX own emulsifying properties whatever the
292 alkenyl chain length and DS. Then, one can notice that the higher the DS (> 6%) or the longer the alkenyl
293 chain length (C16), the higher the density of droplet and the smaller their size (Figure 6 b,d,e). This
294 clearly indicates an improvement of the stabilizing character due to both DS and grafted chain length.
295 Considering the droplet size distribution, particular behaviors are obtained for both XC12(6.3) and
296 XC16(2.2) owning the distribution at D0 and D30 perfectly superimposed with droplets mean and
297 median diameters remaining constant around 10 to 20 μm as indicated in Table 2. Based on these
298 results, one can conclude that HMX specimen allow preparing stable emulsions within the period of
299 time tested as no destabilization was observed within 1 month. Nevertheless, one can notice that slight
300 difference actually exists between microphotographs as some of the droplets of XC12(6.3) emulsion
301 (Figure 6d) have a less spherical shape when compared to those for XC16(2.2) emulsion (Figure 6e).
302 Such a qualitative observation can be explained by the occurrence of flocculation phenomenon. This
303 hypothesis may could be checked on the basis of further analysis such as backscattering data.

304 For the other emulsions analysis, the evolution of the droplet size distribution curves (Figure 6a,b,c)
305 showing a decrease of both median and mean diameter of the droplets (Table 2) reveal that
306 destabilization mechanisms occurred between D0 and D30 mainly by creaming together with a limited
307 phenomenon of flocculation or even the absence of flocculation, this according to the grafting density
308 and the length of the alkyl residue. These latter results and interpretations are in good accordance
309 with the ones discussed in the first section for XC8(4.1).

310 Similar effect of alkenyl chain length was discussed by Kokubun et al. [39], where emulsion droplet size
311 was smaller for DDSA-inulin than OSA-inulin owing equivalent DS. This indicated that longer
312 hydrophobic moieties make it easier polymeric species adsorption onto oil droplets during the
313 homogenization process.

314 If considering the impact of DS, emulsion stability improvement and smaller droplet size were
315 attributed to higher number of hydrophobic moieties as demonstrated by Kokubun et al. [39] and
316 Wang et al. [29] on inulin-OSA/DDSA and Arabic gum-DDSA respectively.



317
318 *Figure 6 : Optical microscopy image at D30 and droplet size distribution at D0 and D30 of the emulsified phase of dispersion*
319 *at 0.2% w/w of different HMX*

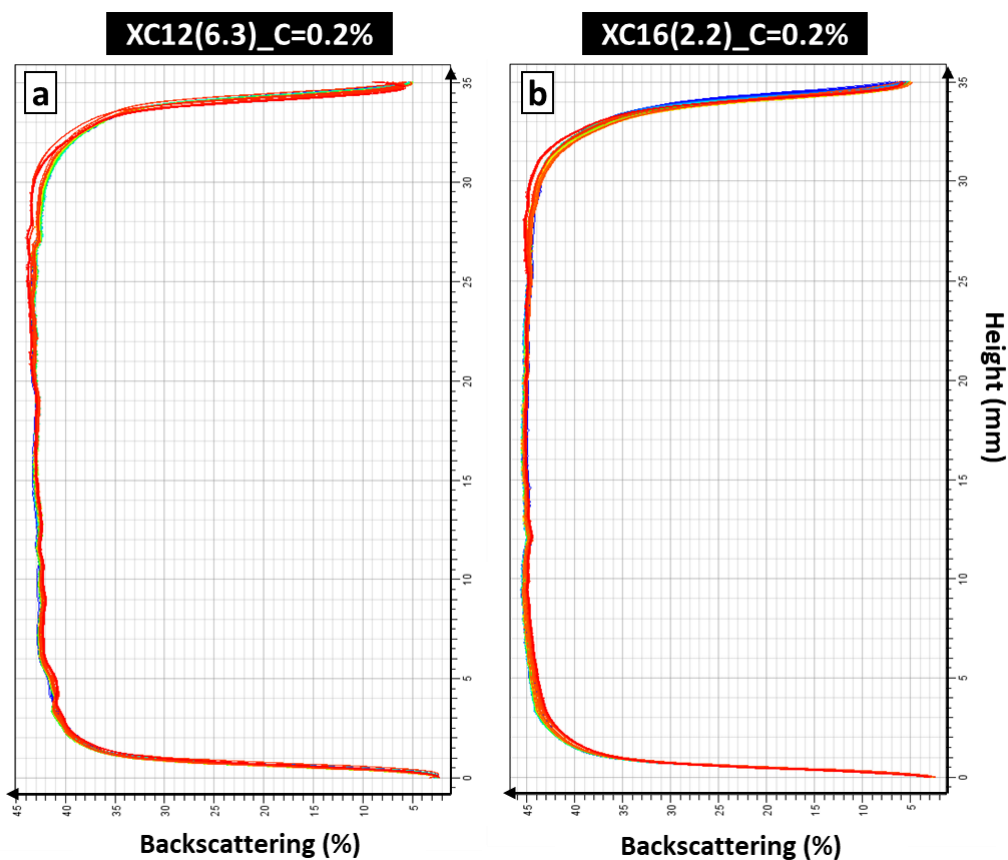
320
321

Table 2 : Median and mean diameter of droplets in the emulsified phase of dispersion at 0.2% w/w of different HMX between D0 and D30

		XC8(4.1)	XC8(6.2)	XC12(2.2)	XC12(6.3)	XC16(2.2)
Median diameter (µm)	D0	126 ± 5	110 ± 2	83 ± 5	22 ± 1	19 ± 1
	D30	105 ± 8	96 ± 16	72 ± 3	20 ± 1	20 ± 1
Mean diameter (µm)	D0	124 ± 5	105 ± 2	70 ± 6	18 ± 1	15 ± 1
	D30	80 ± 8	87 ± 17	63 ± 2	16 ± 1	16 ± 1

322

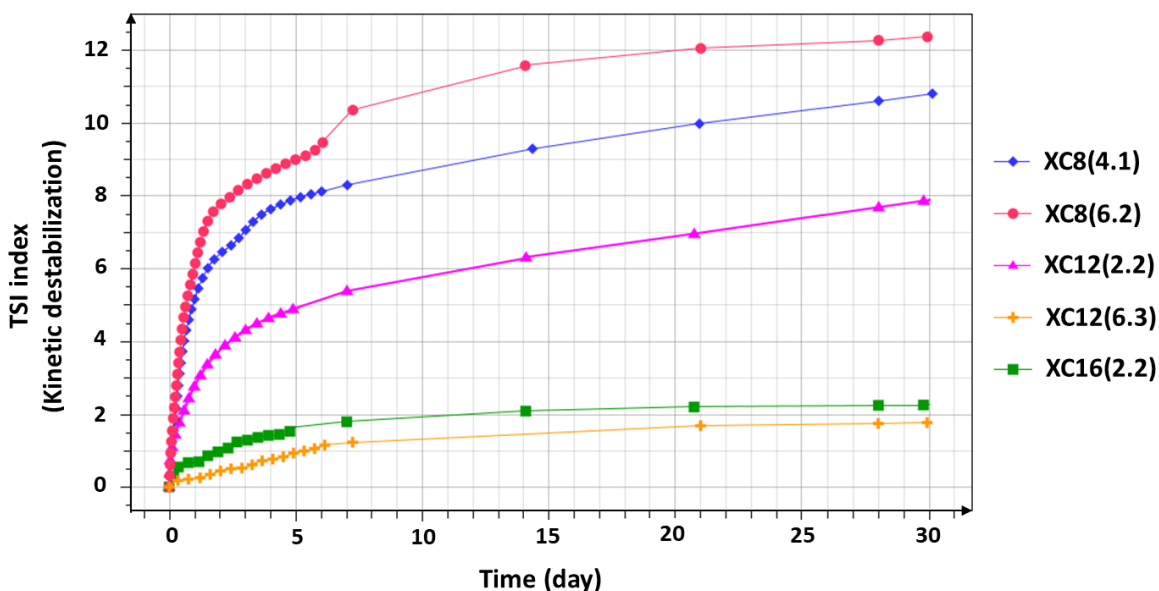
323 Following the same procedure as the one described in section 1, Turbiscan™ characterization of the
 324 different samples was conducted over 1 month. Since the transmission percentage is lower than 0.2%,
 325 the analysis of SMLS was focused on BS signal. Results allowed evidencing two distinct behaviors. The
 326 first one observed for both XC8(6.3) and XC12(2.2) evidenced creaming quite similarly as the profile
 327 obtained for XC8(4.1) (profile not shown - see Figure 4 for comparison). Only slight difference could be
 328 evidenced for the height of the emulsified phase, but the variation clearly remains non-significant. The
 329 second type of profile shows constant BS value which perfectly superimposes on the entire height of
 330 the sample over the whole period of sample monitoring (Figure 7a,b) corresponding to XC12(6.3) and
 331 XC16(2.2), respectively. Same results were observed for XC12(16.9) (data not shown). Thus, no
 332 destabilization occurs and a relatively high and constant opacity (BS = 43-45%) is observed for these
 333 last samples thus illustrating without any doubt the occurrence of highly stable emulsions.



334
335
336

Figure 7 : Raw backscattering data obtained by following the evolution with time of the destabilization of the emulsion formed with: a) XC12(6.3) or b) XC16(2.2) at 0.2% w/w. Samples were scanned over 30 days with different scan periods

337 In addition to the results exposed and discussed above, further parameter could be analyzed from
 338 Turbiscan™ data, namely the destabilization kinetic of the system as evidenced through the evolution
 339 of TSI index as a function of time. According to Figure 8, a relatively fast destabilization occurs even
 340 from the first hours after preparation for emulsions defined as unstable after one month.
 341 Nevertheless, TSI evolution appears slower for HMX owning high DS or long alkenyl grafted moieties
 342 as in these latter cases a low index value ($TSI \leq 2$) is observed over 1 month when compared to HMX
 343 owning low DS and short alkenyl residues.



344 *Figure 8: Evolution of the destabilization kinetic represented by the TSI index for emulsion at 0.2% w/w of different HMX*
 345

346 Based on all results of this second section, both parameters: DS and alkenyl chain length appear
 347 essential as they sharply govern the emulsions kinetic stability. In fact, the goal for preparing stable
 348 emulsion can be achieved using two modified xanthan categories, the dodecyl grafted xanthan as
 349 far as it owns a minimum DS value (over 6%) on the one hand, the hexadecyl grafted xanthan even
 350 at low DS due to long hydrophobic moieties on the second hand. These results are directly related to
 351 the surface-active properties, as previously reported for such HMX owning sufficient DS and/or longer
 352 alkenyl chains, both demonstrated as the most effective in reducing the surface tension [31]. In
 353 addition, such a higher stability may also be facilitated by a negatively more charged polysaccharide
 354 due to the presence of anionic carboxylate groups in the linkage between alkenyl chains and the
 355 xanthan backbone, this providing repulsive forces between the oil droplets, preventing their
 356 aggregation [27,40,41].

357 It is important to note that all attempts to get stable emulsions with using octenyl grafted xanthan
 358 failed even when using HMX owning high DS (up to 6.2%). Thus, in order to improve the emulsion
 359 stability, attempts to investigate the effect of HMX concentration on the one hand and the impact of
 360 the presence of native xanthan as thickening agent on the other hand were investigated and exposed
 361 in the last section of the paper.

362 3.3. Impact of HMX concentration and effect of synergy between native and modified xanthan

363 In this third section, XC8(4.7) was used to investigate on the one hand the effect of concentration by
 364 increasing from 0.2 to 0.5% w/w and on the other the effect of adding 0.1% w/w of native xanthan

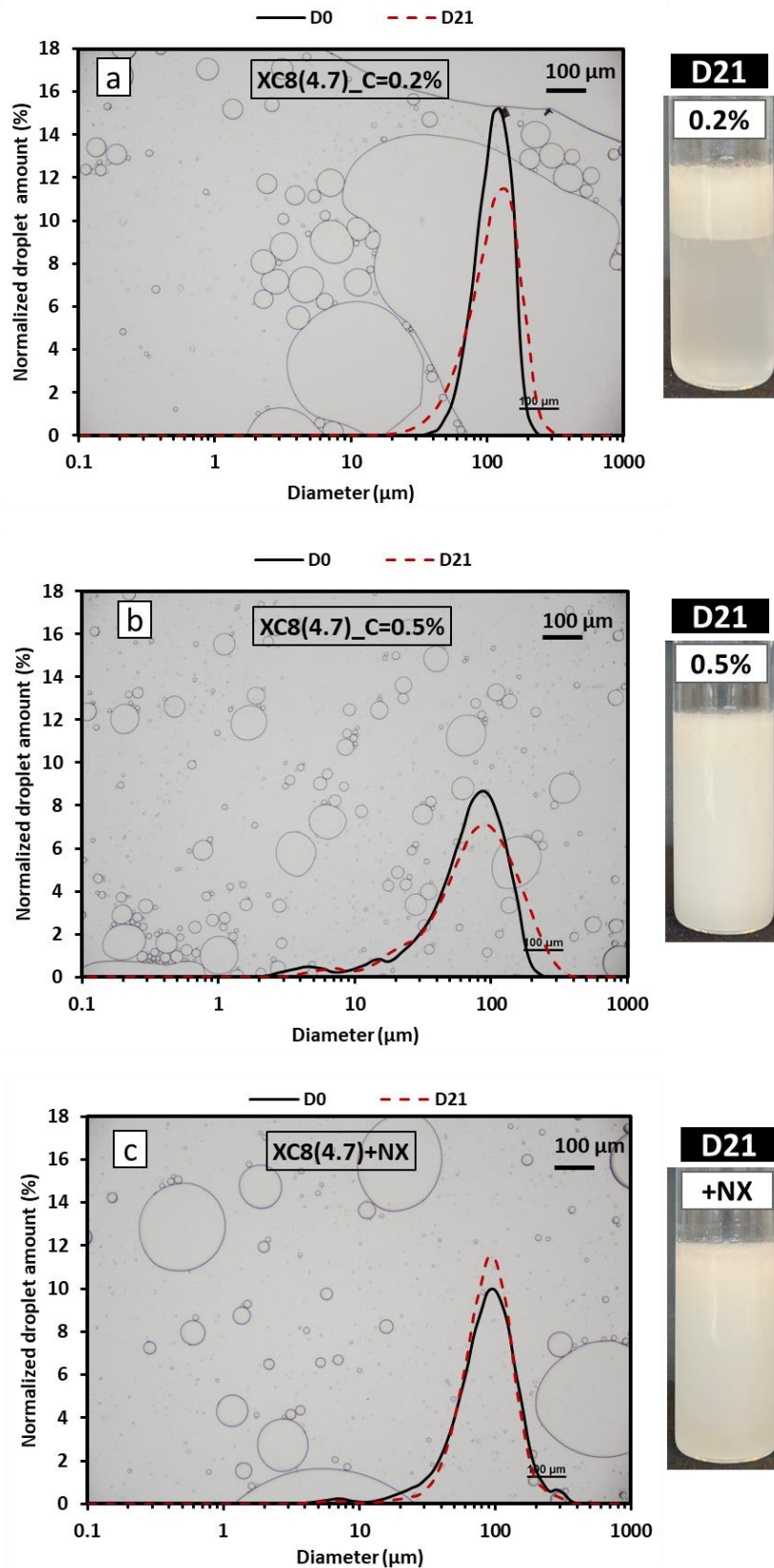
365 (NX) as thickener in emulsion containing 0.2% w/w of XC8(4.7) as emulsifying agent. In this section
366 emulsions were monitored for several weeks.

367 Figure 9 presents the macroscopic aspect for the mixtures corresponding to XC8(4.7) at 0.2% w/w
368 (Figure 9.a), XC8(4.7) at 0.5% w/w (Figure 9.b) and mixture prepared with combining XC8(4.7) at 0.2%
369 w/w + Native Xanthan at 0.1% w/w (Figure 9.c). The first one (a) shows no more than $\frac{1}{3}$ of the height
370 for the emulsified phase as it was demonstrated in the previous sections. Then, mixtures prepared
371 with increasing HMX concentration to 0.5% are characterized by an entire emulsification remaining
372 stable after several weeks. Same behavior was observed for XC8(4.7) at 0.2% w/w + Native Xanthan
373 (c) system from a macroscopic point of view. Thus, both parameters undoubtedly have marked positive
374 impact on the stability of the dispersions.

375 In addition, photographs corresponding to D21 superimposed on the granulometric distribution as
376 represented in Figure 9 bring additional information. Afterwards, micrographs show smaller droplets
377 at D21 for emulsions prepared with lonely HMX additive; the higher the HMX content the smaller the
378 droplets of the emulsified phase. Same tendency but in a lesser extent is observed with addition native
379 xanthan. This is confirmed by a droplets size distribution owning smaller droplets and with lower
380 median diameter for corresponding emulsions at both D0 and D21 as visible in Table 3.

381

382



383
384
385

Figure 9 : Photographs at D21, optical microscopy image at D21 and droplet size distribution at D0 and D30 of the emulsified phase of dispersion at different formulation conditions containing XC8(4.7)

386
387
388

Table 3 also gives the evolution over time of mean diameter for each sample. Again, it is obvious that droplets obtained directly after the preparation protocol (D0), are smaller when either adding NX or increasing the HMX concentration, thus illustrating more efficient emulsification. This is consistent

389 with results obtained elsewhere on OSA-soy polysaccharide [42], inulin-OSA/DDSA [39], OSA-Arabic
 390 gum [29,43], and OSA-starch [25,43]. Authors evidenced a droplet size decreasing when increasing
 391 the derivative polymer concentration. This was explained as the consequence of higher polymer
 392 concentration that makes more emulsifying species available to quickly adsorb on the oil droplets and
 393 cover their surface during the homogenization process, thus preventing flocculation.

394 Then, it was possible to demonstrate that adding NX gives the best stability of mean and median
 395 diameter showing constant values 21 days after the emulsion preparation, this is consistent with
 396 qualitative results described by Fantou et al. [44] on the positive effect of mixing xanthan grafted by
 397 octylamine hydrophobic chains with its pristine xanthan in emulsions stabilization.

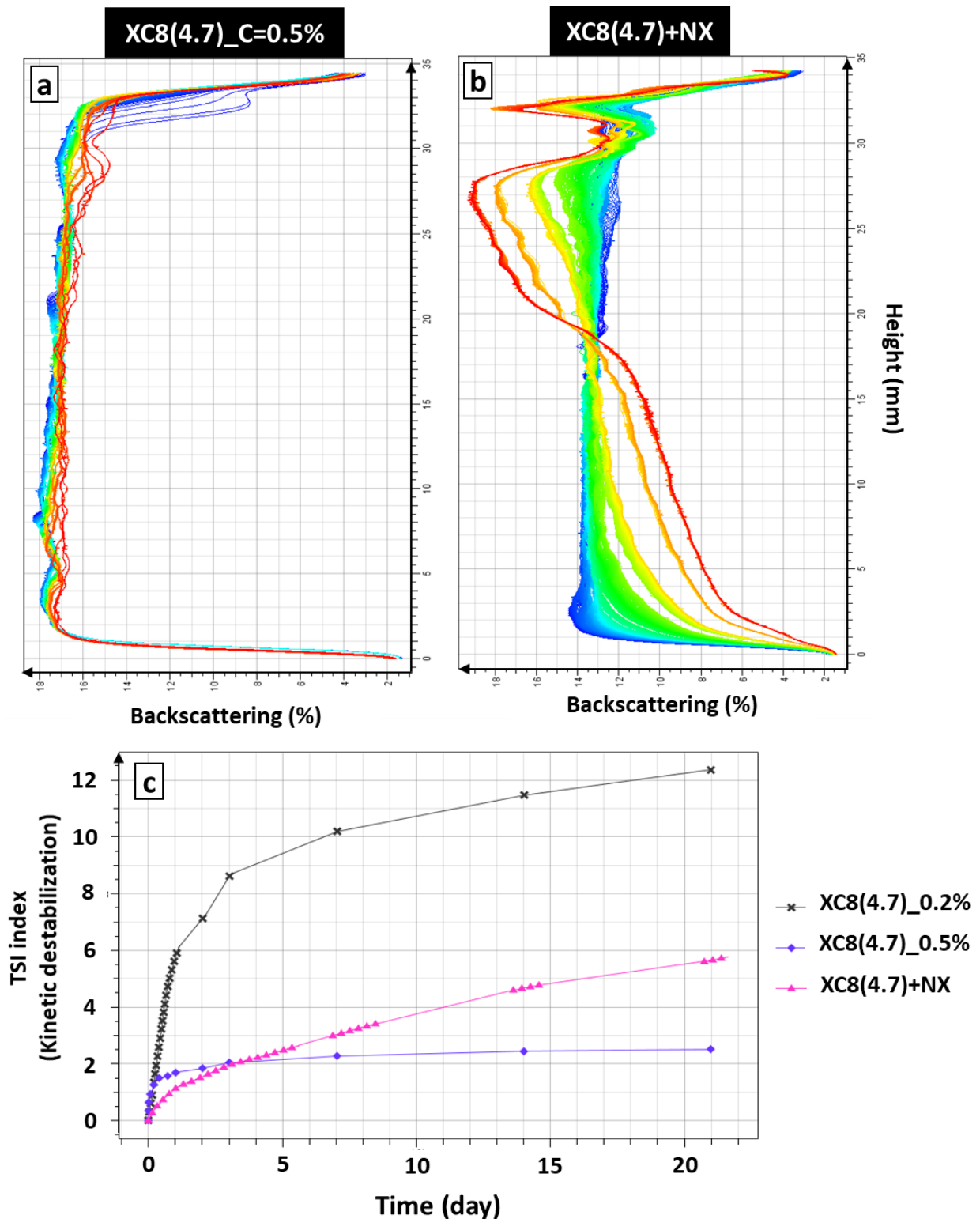
398 *Table 3: Median and mean diameter of droplets in the emulsified phase of dispersion at different formulation conditions*
 399 *containing XC8(4.7) at D0 and D21*

		XC8(4.7)-C=0.2%	XC8(4.7)-C=0.5%	XC8(4.7)-NX
Median diameter (μm)	D0	106 ± 5	70 ± 6	83 ± 4
	D21	109 ± 15	76 ± 3	83 ± 3
Mean diameter (μm)	D0	103 ± 6	59 ± 5	78 ± 6
	D21	94 ± 2	68 ± 2	79 ± 2

400 Thus, as a synergy between the emulsifying agent (HMX) and the thickener one (NX) may play a
 401 valuable role for stabilizing dispersion. Backscattering experiments and TSI data were investigated and
 402 considered to bring a better understanding of the parameters responsible for such effects.
 403 Corresponding results are reported in Figure 10.

404 For XC8(4.7) at 0.2% w/w content backscattering profile is identical to the one presented in the first
 405 section (Figure 4), with highlighting the main occurrence of both creaming and flocculation
 406 phenomenon. Then, one can notice that when increasing the HMX concentration from 0.2 to 0.5%, the
 407 BS remains globally constant for the whole height of the sample over the entire period of time (Figure
 408 10a). Nevertheless, the absence of perfect superposition for the BS curves may be explained by the
 409 presence of large droplets due to local flocculation/coalescence mechanisms without significant
 410 creaming migration. Such hypothesis is consistent with the slight increase of both mean and median
 411 diameter observed over time (Table 3). From a general point of view, BS profile allows establishing
 412 stabilization effect when increasing HMX content, in good accordance with both macroscopic and
 413 microstructure aspects.

414 Finally, if considering the third mixture prepared with HMX/NX combination, one can notice that there
 415 is hardly no agreement depending on whether the macroscopic or microscopic aspect is considered;
 416 thereby, BS evolution clearly evidences a creaming destabilization profile (Figure 10b). However, one
 417 can notice that the destabilization is actually sharply slowed down when compared to the referent
 418 emulsion without NX. In fact, a progressive decrease of BS signal for the lower phase is observed at the
 419 same time as the increase of BS signal for the upper phase. Indeed, the migration of droplets from the
 420 bottom to the top is significantly slowed down when compared to the one in the absence of NX. Thus,
 421 despite a macroscopically fully emulsified appearance, BS data allowed revealing a lonely phenomenon
 422 of slow creaming rather than a long-term stabilization., Finally, TSI index was considered as a tool to
 423 better evidence the differences in the kinetic of destabilization for the three mixtures studied in this
 424 paragraph; corresponding graphs are as presented in Figure 10c. This parameter was followed up
 425 immediately after the mixture was prepared and monitored for a period of 21 days.



426

427 *Figure 10: Raw backscattering data (a, b) and TSI index (c) obtained by following the evolution over 21 days of three type of*
 428 *emulsion containing XC8(4.7); the samples were scanned with different scan periods*

429 One can first notice that TSI evolution corresponding to the basic emulsion (C = 0.2%) shows a sharp
 430 TSI increase within the first 24 hours after the mixture preparation, after which the increase becomes
 431 less rapid but does not tend to stabilize after 21 days. It is interesting to note that TSI index for this
 432 mixture remains higher than the others on the entire period of time considered. At the same time, the

433 addition of NX clearly slows down the destabilization of the mixture with a lower TSI over the whole
434 duration of the study thus highlighting the main action of native xanthan which acts as a thickener
435 delaying the destabilization. Finally, the evolution of TSI corresponding to the emulsion owing the
436 higher HMX content presents a marked tendency to reach an almost constant value (# 2.5) reflecting
437 a stable emulsion; this latter result undoubtedly allows demonstrating the efficacy for amphiphilic
438 xanthan derivatives for the stabilization of O/W emulsions provided there is a sufficient quantity.

439 Same effects were observed with considering dodecyl grafted xanthan owning a low grafting rate
440 (4.8%) (results not shown in the paper). In summary, it can be concluded that increasing HMX
441 concentration or adding NX can be considered as efficient solutions to improve O/W emulsion stability
442 over time.

443 **4. Conclusion**

444 In the current work, emulsifying properties of a series of hydrophobically modified xanthan (HMX)
445 have been studied in order to better understand the phenomenon governing the O/W emulsions
446 stability. HMX was obtained via grafting onto xanthan different alkenyl chain length, namely octenyl,
447 dodecyl and hexadecyl with grafting densities (DS) up to 16%. First, this work allowed establishing
448 that as amphiphilic polysaccharide derivatives, HMX do own emulsifying properties to stabilize water-
449 oil interfaces while native xanthan do not due to their poor interfacial properties as non-absorbing
450 polymers. High stable emulsions were obtained with HMX grafted either by long alkenyl moieties
451 (XC16) even at low grafting density or by medium chain length (XC12) as far as a minimum DS is used
452 (>6%). These latter HMX allowed getting the best emulsion stability with white and homogeneous
453 aspect, constant size distribution, smaller droplets and constant backscattering profile over one
454 month. Such a promising result can be explained by (1) the effectiveness of HMXs in reducing surface
455 tension and (2) to their increased negative charges due to carboxylate groups providing repulsive
456 forces between droplets thus preventing their aggregation. On the contrary, emulsions prepared with
457 using octenyl grafted xanthan showed destabilization through creaming phenomenon; in this case, it
458 was possible to improve emulsion stability by increasing HMX content, thus providing more
459 amphiphilic chains available to coat oil droplets and prevent creaming. Additional experiments allowed
460 demonstrating that another option to improve the stability of O/W emulsions was mixing HMX and
461 native xanthan together, the latter markedly acting as a thickener for the continuous aqueous phase
462 thus slowing down the creaming of oil droplets. To summarize, the whole of this work undoubtedly
463 brings original knowledge on the role and mechanisms of action of hydrophobically modified xanthan
464 in the stabilization of Oil-in-Water emulsions. The promising and effective emulsifying capacities of
465 biosourced amphiphilic xanthan obtained under green modification synthesis was demonstrated, what
466 offers promising potential for industrial applications. Further investigations are now in progress with
467 the particular aims (1) to elucidate the partitioning of HMX molecules between the bulk aqueous phase
468 and O/W interface and (2) to better understanding the reason for the creaming phenomenon.

469 **Acknowledgments**

470 Authors acknowledge the Region Normandie (Agreement 19E00776) and FEDER for grant and financial
471 support.

472

- 474 [1] I. Klojdová, J. Štětina, Š. Horáčková, W/O/W Multiple Emulsions as the Functional
475 Component of Dairy Products, *Chemical Engineering & Technology*. 42 (2019) 715–727.
476 <https://doi.org/10.1002/ceat.201800586>.
- 477 [2] A. Azeem, M. Rizwan, F.J. Ahmad, Z.I. Khan, R.K. Khar, M. Aqil, S. Talegaonkar, Emerging
478 Role of Microemulsions in Cosmetics, *Recent Patents on Drug Delivery & Formulation*. 2
479 (2008) 275–289.
- 480 [3] Barkat Ali Khan, Basics of pharmaceutical emulsions: A review, *Afr. J. Pharm. Pharmacol.*
481 5 (2011). <https://doi.org/10.5897/AJPP11.698>.
- 482 [4] L.A. Trujillo-Cayado, M.C. García, J. Santos, J.A. Carmona, M.C. Alfaro, Progress in the
483 Formulation of Concentrated Ecological Emulsions for Agrochemical Application Based
484 on Environmentally Friendly Ingredients, *ACS Sustainable Chem. Eng.* 5 (2017) 4127–
485 4132. <https://doi.org/10.1021/acssuschemeng.7b00106>.
- 486 [5] T.F. Tadros, *Emulsion Science and Technology: A General Introduction*, in: *Emulsion
487 Science and Technology*, John Wiley & Sons, Ltd, 2009: pp. 1–56.
488 <https://doi.org/10.1002/9783527626564.ch1>.
- 489 [6] M.M. Robins, Emulsions — creaming phenomena, *Current Opinion in Colloid & Interface
490 Science*. 5 (2000) 265–272. [https://doi.org/10.1016/S1359-0294\(00\)00065-0](https://doi.org/10.1016/S1359-0294(00)00065-0).
- 491 [7] J. Sjöblom, *EMULSIONS AND EMULSION STABILITY*, Taylor & Francis, 2006.
492 [http://www.scientificspectator.com/documents/surfactant%20spectator/Emulsions%20
493 and%20Emulsion%20Stability.pdf](http://www.scientificspectator.com/documents/surfactant%20spectator/Emulsions%20and%20Emulsion%20Stability.pdf).
- 494 [8] A. Paraskevopoulou, D. Boskou, V. Kiosseoglou, Stabilization of olive oil – lemon juice
495 emulsion with polysaccharides, *Food Chemistry*. 90 (2005) 627–634.
496 <https://doi.org/10.1016/j.foodchem.2004.04.023>.
- 497 [9] J.-L. Salager, *SURFACTANTS Types and Uses*, FiRP, UNIVERSIDAD DE LOS ANDES-Mérida-
498 Venezuela, 2002. <http://www.nanoparticles.org/pdf/Salager-E300A.pdf>.
- 499 [10] Y. Chevalier, M.-A. Bolzinger, Emulsions stabilized with solid nanoparticles: Pickering
500 emulsions, *Colloids and Surfaces A: Physicochemical and Engineering Aspects*. 439 (2013)
501 23–34. <https://doi.org/10.1016/j.colsurfa.2013.02.054>.
- 502 [11] E. Dickinson, Hydrocolloids at interfaces and the influence on the properties of dispersed
503 systems, *Food Hydrocolloids*. 17 (2003) 25–39. [https://doi.org/10.1016/S0268-
504 005X\(01\)00120-5](https://doi.org/10.1016/S0268-005X(01)00120-5).
- 505 [12] Y. Lu, W. Kang, J. Jiang, J. Chen, D. Xu, P. Zhang, L. Zhang, H. Feng, H. Wu, Study on the
506 stabilization mechanism of crude oil emulsion with an amphiphilic polymer using the β -
507 cyclodextrin inclusion method, *RSC Adv.* 7 (2017) 8156–8166.
508 <https://doi.org/10.1039/C6RA28528G>.
- 509 [13] E. Rotureau, M. Leonard, E. Marie, E. Dellacherie, T.A. Camesano, A. Durand, From
510 polymeric surfactants to colloidal systems (1): Amphiphilic dextrans for emulsion
511 preparation, *Colloids and Surfaces A: Physicochemical and Engineering Aspects*. 288
512 (2006) 131–137. <https://doi.org/10.1016/j.colsurfa.2006.01.044>.
- 513 [14] A.K. Ray, P.B. Bird, G.A. Iacobucci, B.C. Clark, Functionality of gum arabic. Fractionation,
514 characterization and evaluation of gum fractions in citrus oil emulsions and model
515 beverages, *Food Hydrocolloids*. 9 (1995) 123–131. [https://doi.org/10.1016/S0268-
516 005X\(09\)80274-9](https://doi.org/10.1016/S0268-005X(09)80274-9).

- 517 [15] D.R. Underwood, P.S.J. Cheetham, The isolation of active emulsifier components by the
518 fractionation of gum talha, *Journal of the Science of Food and Agriculture*. 66 (1994) 217–
519 224. <https://doi.org/10.1002/jsfa.2740660217>.
- 520 [16] E.J. Vernon-Carter, R. Pedroza-Islas, C. i. Beristain, Stability of Capsicum Annuum
521 Oleoresin-in-Water Emulsions Containing Prosopis and Acacia Gums, *Journal of Texture*
522 *Studies*. 29 (1998) 553–567. <https://doi.org/10.1111/j.1745-4603.1998.tb00183.x>.
- 523 [17] N. Garti, D. Reichman, Surface properties and emulsification activity of galactomannans,
524 *Food Hydrocolloids*. 8 (1994) 155–173. [https://doi.org/10.1016/S0268-005X\(09\)80041-](https://doi.org/10.1016/S0268-005X(09)80041-6)
525 6.
- 526 [18] Y. Wu, W. Cui, N.A.M. Eskin, H.D. Goff, An investigation of four commercial
527 galactomannans on their emulsion and rheological properties, *Food Research*
528 *International*. 42 (2009) 1141–1146. <https://doi.org/10.1016/j.foodres.2009.05.015>.
- 529 [19] N. Garti, Z. Madar, A. Aserin, B. Sternheim, Fenugreek Galactomannans as Food
530 Emulsifiers, *LWT - Food Science and Technology*. 30 (1997) 305–311.
531 <https://doi.org/10.1006/fstl.1996.0179>.
- 532 [20] A.R. Sav, T.A. Meer, R.A. Fule, P.D. Amin, Investigational Studies on Highly Purified
533 Fenugreek Gum as Emulsifying Agent, *Journal of Dispersion Science and Technology*. 34
534 (2013) 657–662. <https://doi.org/10.1080/01932691.2012.683983>.
- 535 [21] L.M. Landoll, Nonionic polymer surfactants, *Journal of Polymer Science: Polymer*
536 *Chemistry Edition*. 20 (1982) 443–455. <https://doi.org/10.1002/pol.1982.170200218>.
- 537 [22] M. Hennock, R.R. Rahalkar, P. Richmond, Effect of Xanthan Gum Upon the Rheology and
538 Stability of Oil-Water Emulsions, *Journal of Food Science*. 49 (1984) 1271–1274.
539 <https://doi.org/10.1111/j.1365-2621.1984.tb14968.x>.
- 540 [23] E. Liwarska-Bizukojc, K. Miksch, A. Malachowska-Jutysz, J. Kalka, Acute toxicity and
541 genotoxicity of five selected anionic and nonionic surfactants, *Chemosphere*. 58 (2005)
542 1249–1253. <https://doi.org/10.1016/j.chemosphere.2004.10.031>.
- 543 [24] E. Olkowska, Ż. Polkowska, J. Namieśnik, Analytics of Surfactants in the Environment:
544 Problems and Challenges, *Chem. Rev.* 111 (2011) 5667–5700.
545 <https://doi.org/10.1021/cr100107g>.
- 546 [25] L.A. Bello-Pérez, C.A. Bello-Flores, M. del C. Nuñez-Santiago, C.P. Coronel-Aguilera, J.
547 Alvarez-Ramirez, Effect of the degree of substitution of octenyl succinic anhydride-
548 banana starch on emulsion stability, *Carbohydrate Polymers*. 132 (2015) 17–24.
549 <https://doi.org/10.1016/j.carbpol.2015.06.042>.
- 550 [26] H.-M. Chen, X. Fu, Z.-G. Luo, Esterification of sugar beet pectin using octenyl succinic
551 anhydride and its effect as an emulsion stabilizer, *Food Hydrocolloids*. 49 (2015) 53–60.
552 <https://doi.org/10.1016/j.foodhyd.2015.03.008>.
- 553 [27] S. Kokubun, I. Ratcliffe, P.A. Williams, The interfacial, emulsification and encapsulation
554 properties of hydrophobically modified inulin, *Carbohydrate Polymers*. 194 (2018) 18–
555 23. <https://doi.org/10.1016/j.carbpol.2018.04.018>.
- 556 [28] G. Li, F. Zhu, Physicochemical, rheological, and emulsification properties of nonenyl
557 succinic anhydride (NSA) modified quinoa starch, *International Journal of Biological*
558 *Macromolecules*. (2021). <https://doi.org/10.1016/j.ijbiomac.2021.10.199>.
- 559 [29] H. Wang, P.A. Williams, C. Senan, Synthesis, characterization and emulsification
560 properties of dodecenyl succinic anhydride derivatives of gum Arabic, *Food*
561 *Hydrocolloids*. 37 (2014) 143–148. <https://doi.org/10.1016/j.foodhyd.2013.10.033>.

- 562 [30] S. Plate, S. Diekmann, U. Steinhäuser, S. Drusch, Determination of the degree of
563 substitution of hydrolysed octenylsuccinate-derivatised starch, *LWT - Food Science and*
564 *Technology*. 46 (2012) 580–582. <https://doi.org/10.1016/j.lwt.2011.12.014>.
- 565 [31] M. Abou Dib, N. Hucher, E. Gore, M. Grisel, Original tools for xanthan hydrophobization
566 in green media: Synthesis and characterization of surface activity, *Carbohydrate*
567 *Polymers*. 291 (2022) 119548. <https://doi.org/10.1016/j.carbpol.2022.119548>.
- 568 [32] C. Fantou, S. Comesse, F. Renou, M. Grisel, Hydrophobically modified xanthan:
569 Thickening and surface active agent for highly stable oil in water emulsions,
570 *Carbohydrate Polymers*. 205 (2019) 362–370.
571 <https://doi.org/10.1016/j.carbpol.2018.10.052>.
- 572 [33] C. Chauvierre, D. Labarre, P. Couvreur, C. Vauthier, A new approach for the
573 characterization of insoluble amphiphilic copolymers based on their emulsifying
574 properties, *Colloid Polym Sci*. 282 (2004) 1097–1104. [https://doi.org/10.1007/s00396-](https://doi.org/10.1007/s00396-003-1040-9)
575 [003-1040-9](https://doi.org/10.1007/s00396-003-1040-9).
- 576 [34] Formulation, Turbiscan Tower User Guide 2.0, (2020).
577 <https://formulation.com/product/turbiscan-tower/>.
- 578 [35] O. Mengual, G. Meunier, I. Cayré, K. Puech, P. Snabre, TURBISCAN MA 2000: multiple
579 light scattering measurement for concentrated emulsion and suspension instability
580 analysis, *Talanta*. 50 (1999) 445–456. [https://doi.org/10.1016/S0039-9140\(99\)00129-0](https://doi.org/10.1016/S0039-9140(99)00129-0).
- 581 [36] M. Luo, X. Qi, T. Ren, Y. Huang, A.A. Keller, H. Wang, B. Wu, H. Jin, F. Li, Heteroaggregation
582 of CeO₂ and TiO₂ engineered nanoparticles in the aqueous phase: Application of
583 turbiscan stability index and fluorescence excitation-emission matrix (EEM) spectra,
584 *Colloids and Surfaces A: Physicochemical and Engineering Aspects*. 533 (2017) 9–19.
585 <https://doi.org/10.1016/j.colsurfa.2017.08.014>.
- 586 [37] Y. Cao, E. Dickinson, D.J. Wedlock, Creaming and flocculation in emulsions containing
587 polysaccharide, *Food Hydrocolloids*. 4 (1990) 185–195. [https://doi.org/10.1016/S0268-](https://doi.org/10.1016/S0268-005X(09)80151-3)
588 [005X\(09\)80151-3](https://doi.org/10.1016/S0268-005X(09)80151-3).
- 589 [38] P.A. Gunning, D.J. Hibberd, A.M. Howe, M.M. Robins, Gravitational destabilization of
590 emulsions flocculated by non-adsorbed xanthan, *Food Hydrocolloids*. 2 (1988) 119–129.
591 [https://doi.org/10.1016/S0268-005X\(88\)80010-9](https://doi.org/10.1016/S0268-005X(88)80010-9).
- 592 [39] S. Kokubun, I. Ratcliffe, P.A. Williams, The emulsification properties of octenyl- and
593 dodecanyl- succinylated inulins, *Food Hydrocolloids*. 50 (2015) 145–149.
594 <https://doi.org/10.1016/j.foodhyd.2015.04.021>.
- 595 [40] M. Falkeborg, Z. Guo, Dodecanyl succinylated alginate (DSA) as a novel dual-function
596 emulsifier for improved fish oil-in-water emulsions, *Food Hydrocolloids*. 46 (2015) 10–
597 18. <https://doi.org/10.1016/j.foodhyd.2014.12.011>.
- 598 [41] D.J. McClements, Critical Review of Techniques and Methodologies for Characterization
599 of Emulsion Stability, *Critical Reviews in Food Science and Nutrition*. 47 (2007) 611–649.
600 <https://doi.org/10.1080/10408390701289292>.
- 601 [42] J.-R. Qi, D.-Y. Zhang, R.-X. Zhao, J.-S. Liao, Y. Cao, J. Xiao, Micro- and nano- emulsions
602 based on soluble soy polysaccharide and octenyl succinic anhydride modified soluble soy
603 polysaccharide, *International Journal of Food Science & Technology*. n/a (2020).
604 <https://doi.org/10.1111/ijfs.14947>.
- 605 [43] Z. Wang, D. Ma, L. Gan, X. Lu, Y. Wang, Octenyl succinate esterified gum arabic stabilized
606 emulsions: Preparation, stability and in vitro gastrointestinal digestion, *LWT*. 149 (2021)
607 112022. <https://doi.org/10.1016/j.lwt.2021.112022>.

608 [44] C. Fantou, J. Yoo, S. Comesse, M. Grisel, F. Renou, Synergy between pristine and
609 hydrophobically modified xanthans for stabilizing oil-in-water emulsions, *Colloid and*
610 *Interface Science Communications*. 37 (2020) 100292.
611 <https://doi.org/10.1016/j.colcom.2020.100292>.